

Original Article

Viscosity Bioreducer Temperature and Concentration Effect on Pressure Drop in Extra Heavy Crude Oil

Maria S. Montalvo-Tello¹, Jose I. Anchondo-Perez¹, Evangelina A. Montalvo Rivero^{*1}, Edgardo J. Suárez-Domínguez², Hugo Herrera-Pilotzi², Elena F. Izquierdo-Kulich²

¹Centro de Investigación FADU. Circuito Interior S/N Centro Universitario Sur, Tampico. Tamaulipas. CP

²Havana University,. Zapata y Carlos Tercero. Ciudad de la Habana, Cuba. CP

*¹Corresponding Author : eamontalvo@uat.edu.mx

Received: 05 October 2022

Revised: 14 April 2023

Accepted: 06 May 2023

Published: 25 May 2023

Abstract - Transporting extra-heavy crude is essential in Mexico because many reserves are high-viscosity fluids. For this reason, some improvers are designed, being useful organic formulations interacting with heavy molecules in crude oil. Biodiesel-based products are helpful for Mexican crudes but can be injected directly into pipelines and pre-mixed or preheated. This work aims to analyze how the concentration of the Bio reducer and the temperature of the flow of crude oil + Bio reducer injected influence the behavior of pressure losses during the transport of crude oil from the mixing point, considering the heat losses that occur through the wall of the tube.

Keywords - Bioreducer effect in extra-heavy crude, Oil viscosity reduction, Preheating reducer injection in pipeline.

1. Introduction

Heavy and extra-heavy crudes have a high viscosity, which leads to high extraction and transport costs [1]. To viscosity reducing, various strategies are used, including raising the temperature and using flow improvers [1,3].

Various models can be found to predict the effects of flow improvers on extra-heavy crude [4]. There sophisticated techniques that have been proposed, i.e. to improve the flow of crude oil in a reservoir by removing asphaltenes through ultrasonic means [6] or techniques based mainly on nanotechnologies [7] and organic products such as alkylbenes derivatives [9]. These products depend on the nature of the crude oil being transported [10,12,13]. This work deals with reducing viscosity and, therefore, pressure losses through a combined analysis of both strategies. For better pipeline transport, heating is the traditional viscosity reduction technique, Instead of chemical injection [15,17].

In this paper, an injection scheme is analysed in which a part of the crude to be transported is separated from the mainstream, heated and injected with a flow improver, and mixed with the untreated crude. The outline of the process under study is shown in Figure 1.

This work aims to analyze how the concentration of the Bioreducer and the temperature of the flow of crude oil + Bioreducer injected influence the behavior of pressure losses during the transport of crude oil from the mixing point, considering the heat losses that occur through the wall of the tube.

Figure 1. Schematic of the crude oil transport system under analysis and pre-treatment of the flow before entering the system. T is the temperature, Q is the flow, and x is the volume fraction of the improver in current 0. The subscript a indicates the environment with which the tube is in contact.

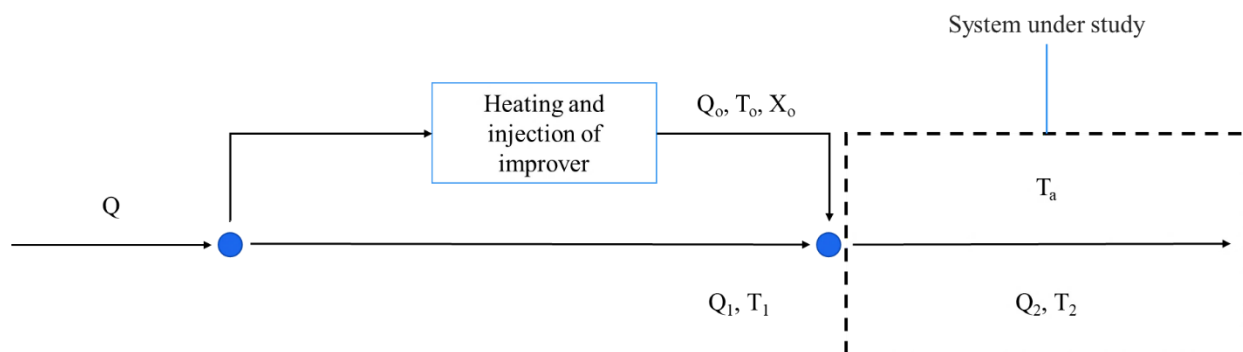


Fig. 1 Outline of the process under study



2. Model

2.1. Obtaining the Model

It proposed correlations related to the flows' physicochemical properties, the macroscopic balance of Mass and energy at the mixing point, and the equations of continuity, quantity of movement, and temperature change, respectively.

2.1.1. Correlations to Determine Physicochemical Properties

The density, viscosity, and heat capacity at the mixing point will depend on the composition and properties of the inlet flow streams. In this case, the following relationships are assumed:

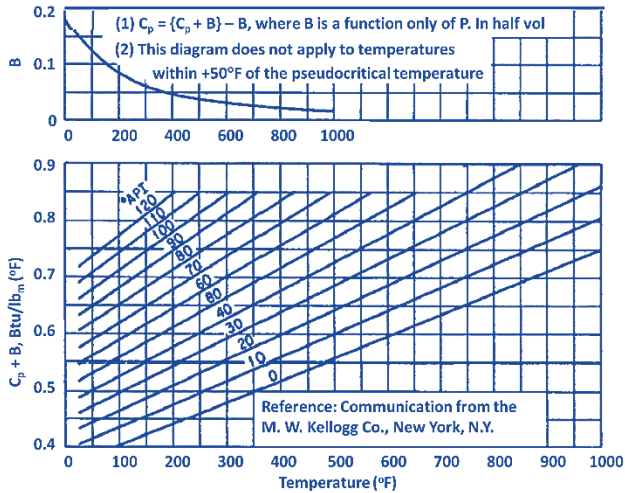


Fig. 2 Empirical estimation of calorific capacity from temperature and API degrees [20]

$$\rho_2 = \left(\frac{1 - y_0}{\rho_1} + \frac{y_0}{\rho_0} \right)^{-1} \tag{1}$$

$$\mu_2 = \exp(y_0 \ln \mu_0 + (1 - y_0) \ln \mu_1) \tag{2}$$

$$C_2 = y_0 C_0 + (1 - y_0) C_1 \tag{3}$$

$$y_0 = \frac{\rho_0 Q_0}{\rho_0 Q_0 + \rho_1 Q_1} \tag{4}$$

μ_0 and μ_1 are viscosities from experimental rheological behaviors. The heat capacity is estimated from the established empirical correlations shown in Figure 2.

2.1.2. Mass and Energy Balance at the Mixing Point

The mass and energy balance at the mixing point makes it possible to determine the flow and inlet temperature of the crude oil transport system under consideration. From this balance, and adequately substituting the correlations related to the physical properties, we obtain:

$$Q_2 = Q_0 + Q_1 \tag{5}$$

$$T_2 = \frac{\rho_0 v_0 C_0 T_0 + \rho_1 (1 - v_0) C_1 T_1}{\rho_0 \rho_1} \frac{\rho_0 + y_0 (\rho_1 - \rho_0)}{C_1 + y_0 (C_0 - C_1)} \tag{6}$$

$$v_0 = \frac{Q_0}{Q_2} \tag{7}$$

2.1.3. Spatial Profiles of Speed and Temperature in the Tube

From the phenomenological equations of transport in coordinates to cylindrical, considering steady state, laminar regime, and Newtonian flow is obtained:

$$\frac{\partial \rho}{\partial t} + \frac{1}{r} \frac{\partial \rho r v_r}{\partial r} + \frac{1}{r} \frac{\partial \rho v_\theta}{\partial \theta} + \frac{\partial \rho v_z}{\partial z} = 0 \tag{8}$$

$$\frac{\partial \rho v_z}{\partial z} = 0 \tag{9}$$

of the equation of quantity of motion:

$$\rho \left(\frac{\partial v_z}{\partial t} + v_r \frac{\partial v_z}{\partial r} + \frac{v_\theta}{r} \frac{\partial v_z}{\partial \theta} + v_z \frac{\partial v_z}{\partial z} \right) = - \frac{\partial p}{\partial z} + \mu \left[\frac{1}{r} \frac{\partial}{\partial r} \left(r \frac{\partial v_z}{\partial r} \right) \right] + \mu \left[\frac{1}{r^2} \frac{\partial^2 v_z}{\partial \theta^2} + \frac{\partial^2 v_z}{\partial z^2} \right] + \rho g_z \tag{10}$$

$$\frac{\partial p}{\partial z} = \mu_2 \frac{1}{r} \frac{\partial}{\partial r} \left(r \frac{\partial v}{\partial r} \right) \tag{11}$$

the temperature change equation, considering that the convective mechanism produces heat transport and that there are heat losses through the tube wall:

$$\rho C_2 V \frac{dT}{dz} = \frac{k}{\delta} (T_a - T) : T_a > T \tag{12}$$

where k is the heat transfer coefficient of the thick tube wall, δT_2 is the spatial average temperature of the fluid at a distance z , and V is the average velocity of the liquid, estimated as:

$$V = \frac{Q_2}{A} \tag{13}$$

where A is the area of the cross-section of the flow.

2.2. Estimation of Pressure Losses

It is established that viscosity μ_2 depends on the average temperature of the fluid and is, therefore, independent of position to simplify the problem. The velocity profile is obtained from the solution of the differential equation:

$$-\Phi = \mu_2 \frac{1}{r} \frac{d}{dr} \left(r \frac{dv}{dr} \right) \tag{14}$$

subject to boundary conditions:

$$\frac{dv}{dr} = 0 : r = 0$$

$$v = 0 : r = R \tag{15}$$

where:

$$\Phi = \frac{dp}{dz} \tag{16}$$

The differential equation (14) has an exact analytic solution, which is:

$$v(r) = \frac{\Phi}{4\mu_2}(R^2 - r^2) \tag{17}$$

Equation (17) represents the spatial velocity profile, where its integration concerning the cross-section of the tube allows obtaining the average velocity:

$$V = \int_0^{2\pi} \int_0^R \left(\frac{\Phi}{4\mu_2}(R^2 - r^2) \right) r dr d\theta$$

$$V = \frac{1}{8}\pi R^4 \frac{\Phi}{\mu_2} \tag{18}$$

In such a way that the behavior of the pressure is expressed through the differential equation:

$$\frac{dp}{dz} = \frac{8}{\pi R^4} V \mu_2 \tag{19}$$

The viscosity depends on the temperature, so if the fluid temperature is greater than the temperature of the environment and heat losses occur, the viscosity value will ultimately depend on the distance z.

From equation (12):

$$\frac{dT}{dz} = \alpha(T_a - T)$$

$$T(0) = T_2 \tag{20}$$

$$T = T_a + (T_2 - T_a) \exp(-z\alpha) \tag{21}$$

where:

$$\alpha = \frac{k}{\delta \rho_2 C_2 V} \tag{22}$$

and temperature T₂ replaces, taking into account equation (6).

The idea is then based on obtaining the equation that describes the dependence of viscosity concerning temperature and improver concentration, for which a statistical adjustment of the experimental results obtained at a laboratory scale associated with the rheology of crude oil is made. In the equation got, equation (21) is then substituted, so the viscosity is explicitly expressed as a function of z. Replacing this relationship in equation (19) and integrating for z yields the behavior of pressure losses.

Results predicted by the model for the transport of ebony crude oil with heating and injection of a biodiesel-base improver

The sample of crude oil ebony has a density of 12 degrees API. The viscosity behavior to temperature and the concentration of bio-reducer obtained at the laboratory scale is shown in Figure 3.

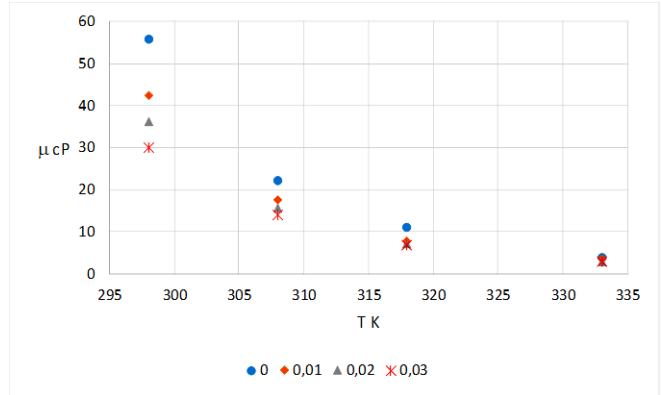


Fig. 3 Experimental behavior of viscosity (cP) for temperature (K) considering as a parameter the concentration of bioreducer.

Statistical multiple regression techniques were applied to the experimental results, obtaining the results shown in Tables 1, 2, and 3.

Since the P value is less than 0.01, there is a statistically significant correlation between the dependent variable (viscosity) and the independent variables (temperature and improver concentration), with a confidence level of 99%. The Durbin-Watson (DW) test results for residue analysis yielded a P value greater than 0.05, so there is no indication of a serial autocorrelation of the residues. The adjusted model is:

$$\mu = (343.7 - 1.02T - 314.7x) \text{ cP} \tag{23}$$

$$\mu = (343.7 - 1.02T - 314.7x) \times 10^{-3} \text{ Pa.s} \tag{24}$$

The fluid will be considered to move through a tube 5 inches in diameter, where:

$$V = 0.1 \frac{m}{s} \tag{25}$$

$$A = \frac{\pi}{4} D^2 = 1.2668 \times 10^{-2} m^2 \tag{26}$$

In such a way that:

$$Q = 1.2668 \times 10^{-3} \frac{m^3}{s}$$

$$= 28914. \frac{\text{gal}}{d}$$

$$= 688.44 \frac{B}{d}$$

It is considered that the density and heat capacity of the crude oil is practically constant for the temperature range analyzed, therefore:

$$API = \frac{141.5}{g} - 131.5$$

$$12 = \frac{141.5}{g} - 131.5 : g = 0.98606$$

$$\rho = 986 \frac{\text{kg}}{\text{m}^3}$$

And that the temperature of the crude oil in current 1 is equal to the ambient temperature:

$$T_1 = 25^\circ\text{C} = 298\text{K}$$

The caloric capacity at the average temperature is estimated in Figure 2:

$$30^\circ\text{C} = 86.0^\circ\text{F}$$

$$C = 0.45 \frac{\text{Btu}}{\text{lb}^\circ\text{F}} = 1884.1 \frac{\text{J}}{\text{kgK}}$$

The outlet temperature of the mixing point, considering that the density and heat capacity of the fluids being mixed is practically the same, depends on the output temperature T_0 of the heating unit and the fraction v_0 of the current one being heated:

$$T_2 = v_0T_0 + (1 - v_0)T_1 \quad (27)$$

The thickness of the tube wall is

$$\delta = 0.0048\text{m}$$

And:

$$T_2 = v_0T_0 + 298(1 - v_0) \quad (28)$$

And it is assumed that the coefficient of heat transfer through the tube wall is:

$$k = 50 \frac{\text{W}}{\text{mK}}$$

Appropriately substituting the obtained relations, the behavior of viscosity is obtained:

$$\mu = 0.03974 - 0.3147x - 0.00102v_0(T_0 - 298) \exp(-0.05z) \text{ Pas} \quad (29)$$

Therefore:

$$\alpha = \frac{k}{\delta\rho_2C_2V}$$

$$= \frac{50 \frac{\text{W}}{\text{m}^2\text{K}}}{0.0048\text{m} \times 986 \frac{\text{kg}}{\text{m}^3} \times 1884.1 \frac{\text{J}}{\text{kgK}} \times 0.1 \frac{\text{m}}{\text{s}}}$$

$$\alpha = 5.6072 \times 10^{-2} \frac{1}{\text{m}}$$

Defining the pressure drop in the system:

$$\Delta P = P_1 - P_L \quad (30)$$

Substituting equation (29) into equation (19) and integrating, one obtains:

$$\Delta P = \int_0^L \left(-\frac{49203}{\pi} (0.3147x + 0.00102v_0e^{-0.05z}(T_0 - 298) - 0.03974) \right) dz \quad (31)$$

The ambient temperature value is considered to be:

$$T_a = 25^\circ\text{C} = 298\text{K}$$

$$\Delta P = (622.40 - 4928.8x)L + v_0(95211. + 319.5T_0(e^{-0.05L} - 1) - 95211e^{-0.05L}) \quad (32)$$

Table 1. Results of the statistical adjustment

Parameter	Dear	Error	T-statistician	Value of p
constant	343. 739	47. 5474	7. 22939	0. 0000
T	-1. 02328	0. 150947	-6. 7791	0. 0000
x	-314. 793	174. 571	-1. 80324	0. 0946

Table 2. Analysis of variance

Fountain	Sum of squares	Gl	Average square	Statistician f	Value of p
model	2999. 21	2	1499. 61	24. 60	0. 0000
waste	792. 347	13	60. 9498		

Table 3. Adjustment results

R square %	79. 1023
R squared (adjusted to GL) %	75. 8873
standard estimate error	7. 80703
absolute mean error	5. 95829
Durbin-Watson statistician	1. 77784 (P=0. 2272)
self-correlation of waste	-0. 12429

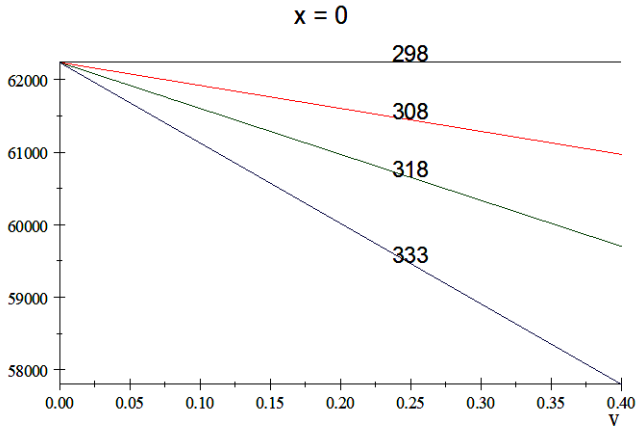


Fig. 4 The behavior of pressure losses ($L = 100$ m) for the volume fraction of the heated flow in the absence of a flow improver, considering as a parameter the outlet temperature

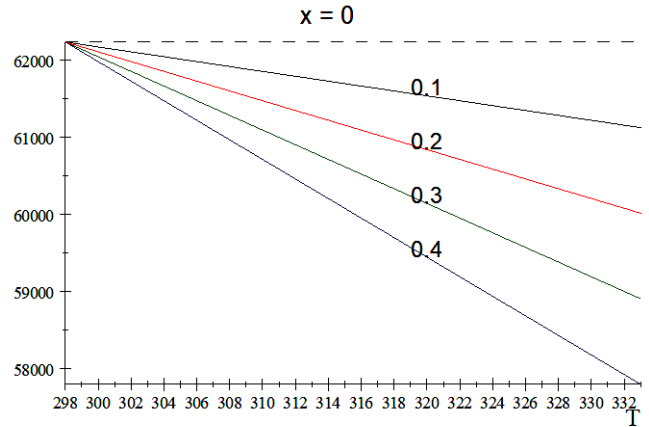


Fig. 6 The behavior of pressure losses concerning temperature ($L = 100$ m) in the absence of an improver considering as a parameter the fraction in the volume of heated crude oil

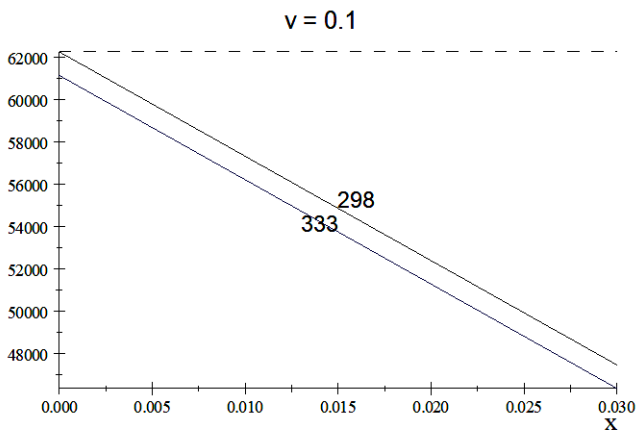


Fig. 5 The behavior of pressure losses ($L = 100$ m) for the volume fraction of the improver injected into the system, considering that the volume fraction of heated crude oil to which the Bio-reducer is injected is equal to 0.1 and considering as a parameter the output temperature of the heating system

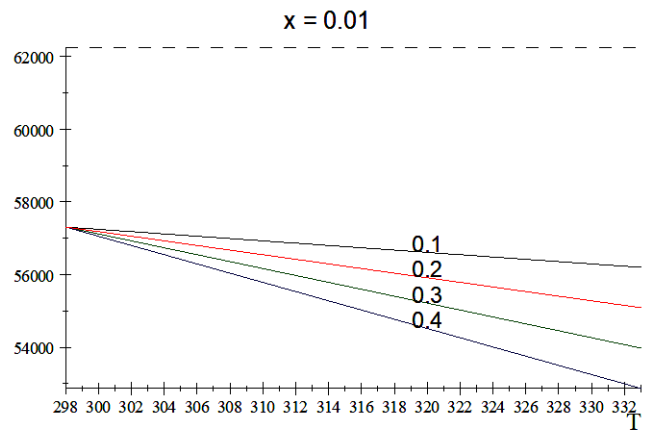


Fig. 7 The behavior of pressure losses to temperature ($L = 100$ m) for a fraction in the volume of improver equal to 0.01 is considered as a parameter of the fraction in the volume of heated crude oil

3. Results and Discussion

3.1. Analysis of Predicted Results

The predicted results were calculated considering a tube of 100 m in length. Figure 4 shows the behavior of pressure losses concerning the volume fraction of the heated flow in the absence of a flow improver. The crude oil outlet temperature of the heating section has been taken as a parameter. Note that pressure losses decrease as the heated fraction is more extensive, and this favorable effect becomes more significant as the temperature increases. Note that for a 298K room temperature, the absence of heating in the system is being considered, so in this figure, it is expected that the pressure losses will show a constant value. In this sense, this will be the more loss obtained in the system, corresponding to the absence of heating and injection of flow improver. For this reason, this value is taken as a reference in the rest of the analyses carried out to visualize this treatment's effect on the operating conditions.

Figure 5 shows the effect of the improver fraction injected into the system with and without heating. In this case, the improver significantly decreases pressure losses, this effect being more remarkable when the temperature is increased.

Figure 6 shows the effect of temperature in the absence of an improver considering the fraction of crude oil heated as a parameter. In this case, pressure losses are predicted to decrease with increasing temperature, and this effect is more significant as the fraction of heated crude increases.

The same behavior is illustrated in Figure 7. Still, the injection of a flow improver has been considered, predicting a more favorable behavior than that obtained without an improver.

4. Conclusion

Pressure losses during crude oil transport depend on the viscosity of the crude oil, so the reduction of these is achieved through processes that decrease thickness. In this work, the most applied methods are heating the fluid and adding chemical additives acting as viscosity reducers. Either of these methods implies an increase in the cost of the process, which is supposed to be compensated economically by decreasing pumping costs or increasing crude oil production for the same pumping pressure. Both methods can be applied in combination. Here, a scheme is proposed based on heating a fraction of the flow to be transported, plus the bio-reducer injected and which is returned into the process, causing a decrease in viscosity. This effect was analyzed

based on the transport of ebony crude oil with an injection of the Biodiesel-base improver, obtaining, as expected, that pressure losses decrease with the increase in temperature, the fraction of heated flow, and the injection of the improver. In this case, the most appropriate option for a given case should be selected, including an economic feasibility study that allows determining the operating condition that maximizes profits or decreases costs.

Acknowledgments

EAMR thanks to the UAT-Invest 2023 project. EJSJ thanks to the PRODEP project for CAEF 2021. JIAP thanks to project 316443.

References

- [1] Ibrahim Raheek, Manal K. Odah, and Amna Al-Mufti, "An Overview on the Recent Techniques for Improving the Flowability of Crude Oil in Pipelines," *IOP Conference Series: Materials Science and Engineering*, vol. 579, p. 012054, 2019. [[CrossRef](#)] [[Google Scholar](#)] [[Publisher Link](#)]
- [2] Karan Dev, and Rajesh Rana, "Force Convective Heat Transfer through MWCNT/Nano Fluids," *SSRG International Journal of Mechanical Engineering*, vol. 3, no. 10, pp. 7-10, 2016. [[CrossRef](#)] [[Publisher Link](#)]
- [3] Farid Souas, Abdelhamid Safri, and Abdelbaki Benmounah, "A Review on the Rheology of Heavy Crude Oil for Pipeline Transportation," *Petroleum Research*, vol. 6, no. 2, pp. 116-136, 2021. [[CrossRef](#)] [[Google Scholar](#)] [[Publisher Link](#)]
- [4] Fayang Jin et al., "An Improved Viscosity Prediction Model of Extra Heavy Oil for High Temperature and High Pressure," *Fuel*, vol. 319, p. 123852, 2022. [[CrossRef](#)] [[Google Scholar](#)] [[Publisher Link](#)]
- [5] D. Sarath Chandra et al., "Impact of Different Volume Concentrations and Flow Rates on the Thermal Performance of Counter flow Cylindrical Shell and Helical Coil Heat Exchanger using Cu/H₂O Nano Fluids," *SSRG International Journal of Thermal Engineering*, vol. 6, no. 3, pp. 11-15, 2020. [[CrossRef](#)] [[Publisher Link](#)]
- [6] Ephraim Otumudia et al., "Effects of Reservoir Rock Pore Geometries and Ultrasonic Parameters on the Removal of Asphaltene Deposition under Ultrasonic Waves," *Ultrasonics Sonochemistry*, vol. 83, p. 105949, 2022. [[CrossRef](#)] [[Google Scholar](#)] [[Publisher Link](#)]
- [7] Shadfar Davoodi et al., "Experimental and Field Applications of Nanotechnology for Enhanced Oil Recovery Purposes: A Review," *Fuel*, vol. 324, p. 124669, 2022. [[CrossRef](#)] [[Google Scholar](#)] [[Publisher Link](#)]
- [8] A. Anish et al., "A Review on Plate Fin Heat Exchanger," *SSRG International Journal of Mechanical Engineering*, vol. 4, no. 4, pp. 33-47, 2017. [[CrossRef](#)] [[Publisher Link](#)]
- [9] Zhichao Zhou et al., "Synthesis of Multi-alkyl Polyamines and Their Performance as Flow Improver in Crude Oil," *Tenside Surfactants Detergents*, 2022. [[CrossRef](#)] [[Google Scholar](#)] [[Publisher Link](#)]
- [10] Jose Antonio Muñoz, and Jorge Ancheyta, "Techno-economic Analysis of Heating Techniques for Transportation of Heavy Crude Oils by Land Pipeline," *Fuel*, vol. 331, p. 125640, 2023. [[CrossRef](#)] [[Google Scholar](#)] [[Publisher Link](#)]
- [11] Lokesh Varma, Suresh Babu Koppula, and N.V.V.S.Sudheer, "Influence of Pressure Drop, Reynolds Number and Temperature in the Design of Double Pipe Heat Exchanger on Hot Fluid Side in Inner Pipe," *SSRG International Journal of Mechanical Engineering*, vol. 4, no. 12, pp. 28-36, 2017. [[CrossRef](#)] [[Publisher Link](#)]
- [12] Farah Ansari et al., "Chemical Additives as Flow Improvers for Waxy Crude Oil and Model Oil: A Critical Review Analyzing Structure-Efficacy Relationships," *Energy Fuels*, vol. 36, no. 7, pp. 3372-3393, 2022. [[CrossRef](#)] [[Google Scholar](#)] [[Publisher Link](#)]
- [13] Osamah Alomair, Adel Elsharkawy, and Alanood Alshammari, "Measurements and Prediction of Heavy and Extra-Heavy Oil Viscosities Considering the Effects of Heat and Solvent Dilution," *SSRN*, 2022. [[CrossRef](#)] [[Google Scholar](#)] [[Publisher Link](#)]
- [14] Ravikiran et al., "Viscosity and Tribological Characteristics of Sunflower Oil with ZnO as Additive," *SSRG International Journal of Mechanical Engineering*, vol. 9, no. 9, pp. 1-7, 2022. [[CrossRef](#)] [[Google Scholar](#)] [[Publisher Link](#)]
- [15] P. Schacht-Hernández et al., "In Situ Upgrading of Heavy Crude Oil: Comparative Study of the Performance of Cu-, Fe-, Ni-, or Zr-Containing Water-Based Catalysts," *Energy Fuels*, vol. 36, no. 20, pp. 12580-12590, 2022. [[CrossRef](#)] [[Google Scholar](#)] [[Publisher Link](#)]
- [16] Edgardo Jonathan Suarez-Dominguez, "Asphaltenes Dispersion by Thermal Change And Petroleum Viscosity: Mesoscopic Model," *SSRG International Journal of Mechanical Engineering*, vol. 8, no. 1, pp. 8-13, 2021. [[CrossRef](#)] [[Google Scholar](#)] [[Publisher Link](#)]

- [17] Simin Tazikeh et al., “A Systematic and Critical Review of Asphaltene Adsorption from Macroscopic to Microscopic Scale: Theoretical, Experimental, Statistical, Intelligent, and Molecular Dynamics Simulation Approaches,” *Fuel*, vol. 329, p. 125379, 2022. [[CrossRef](#)] [[Google Scholar](#)] [[Publisher Link](#)]
- [18] Petrus Tri Bhaskoro et al., “Online Flow Assurance Tool for Optimum Wax Management at Field,” *SPE Annual Technical Conference and Exhibition*, 2022. [[CrossRef](#)] [[Google Scholar](#)] [[Publisher Link](#)]
- [19] Lee Yeh Seng, and Berna Hascakir, “Role of Intermolecular Forces on Surfactant-steam Performance into Heavy Oil Reservoirs,” *SPE Journal*, vol. 26, no. 4, pp. 2318-2323, 2021. [[CrossRef](#)] [[Google Scholar](#)] [[Publisher Link](#)]
- [20] Himmelblau David, *Basic Principles and Calculations in Chemical Engineering*, 6 Edition, Prentice hall, 1997. [[Google Scholar](#)]